HIGH FREQUENCY INVERTER BASED ATMOSPHERIC PRESSURE PLASMA TREATMENT SYSTEM*

C.D. TUDORAN[1,2], V. SURDUCAN[2], A. SIMON[1], A.M PAPIU[1], O.E. DINU[1], S.D. ANGHEL[1]

[1] Faculty of Physics, Babes-Bolyai University, Cluj-Napoca, M. Kogalniceanu 1, RO-400084, Romania
[2]National Institute for Research and Development of Isotopic and Molecular Technologies, 65-103 Donath Str., 400293, Cluj-Napoca, Romania
E-mail: cristian.tudoran@itim-cj.ro

Received September 5, 2011

The work presents a new laboratory-made atmospheric pressure plasma treatment system based on a modern half-bridge type inverter circuit (1.71 MHz, 200 W) combined with a Tesla resonator. The cold non-thermal plasma is generated in flowing helium. It was characterized and was tested for surfaces treatment.

Key words: cold atmospheric pressure plasma, half-bridge type inverter, optical emission, surface treatment.

1. INTRODUCTION

Atmospheric Pressure Plasmas (APPs) have shown great promise when applied to change the surface properties of materials: friction, wettability, adhesion, gas and fluid permeability, bio-compatibility, corrosion, wear and scratch resistance and dye-affinity. APPs can be operated to obtain a cold gas discharges with the aim to avoid a strong thermal transfer to the substrates exposed to the plasma. The surface treatment at atmospheric pressure is simpler to set-up, easier and economical to operate and more productive, compared to traditional low pressure plasma treatment.

Within the different types of atmospheric pressure non-thermal plasmas, *Dielectric Barrier Discharges* (DBDs) are the most interesting solution. They have been widely used in industrial applications like ozone generators, plasma display panels, volatile organic compounds destruction and surface modifications. The plasma-surface interaction is a rather complicate process which involves several complex chemical and physical mechanisms. For this reason, plasma processing is

* Paper presented at the 12th International Balkan Workshop on Applied Physics, July 6–8, 2011, Constanta, Romania.

the subject of study in many research areas like plasma physics, surface science, gas-phase chemistry and atomic and molecular physics. The common theme is the generation and use of plasmas to activate a chain of chemical reactions at a substrate surface. In this work a new AP-DBD generator is presented, as a continuation of our last laboratory made APP sources [1–3].

2. RF HIGH VOLTAGE GENERATOR

2.1. RF POWER SOURCE – A SERIES RESONANT INVERTER

The classic voltage-fed half-bridge series resonant inverter was firstly introduced by Baxandall [4]. It consists of a half-bridge inverter with a series $L_1C_1R_1$ circuit connected to the midpoint M (Fig. 1a). In order to obtain tuned series resonant operation, the switching frequency of the inverter is set to be equal to the resonant frequency of the *LCR* load. Inverters normally supply power to loads that are a combination of a resistance and an inductance, such as electric motors, transformers, etc. This combination inductance-resistance gives rise to a quasi-triangular wave shape current flowing through the load.

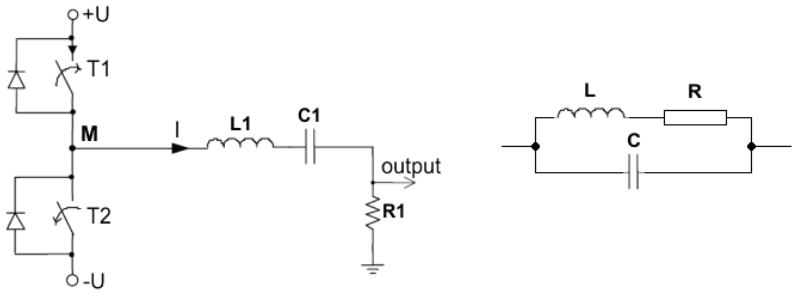

(a) (b)

Fig. 1 – The basic voltage-fed series resonant inverter.

When instead of $L_1C_1R_1$ load, in the midpoint M is connected a Tesla coil, the inverter is supplying power to a load consisting of a *LR* series circuit in parallel with *C* (Fig.1b), were *L*, *C* and *R* represent the inductance, the self capacitance and the loss resistance of the coil, respectively. This circuit has a self-resonant frequency, $f_o = 1/\left(2\pi\sqrt{LC}\right)$, also called "natural frequency". Driving this load with a square voltage waveform having the same frequency as its self-resonant frequency, it will result in a sinusoidal current flowing through it. The square voltage waveform contains the fundamental frequency and all of the odd harmonics of this frequency, but the resonant load only select the fundamental frequency. Unlike coils commonly used in the power electronics or RF engineering, Tesla coil

has a low loss-resistance and consequently a high quality factor $Q = \sqrt{L}/(R\sqrt{C})$. High-Q circuits have the quality to store up high energy over time and then to transfer it to another load. In our case, this load will be the plasma chamber filled or not with plasma.

The block diagram of our inverter based plasma source is given in Fig. 2.

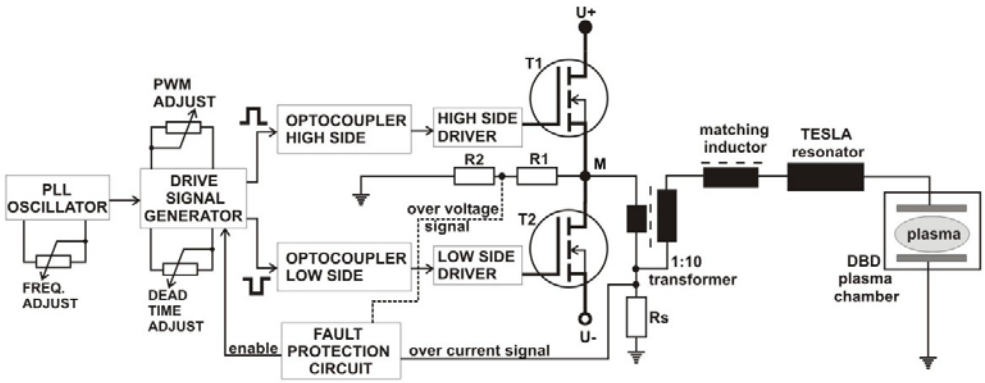

Fig. 2 – The inverter based plasma source block diagram.

The PLL oscillator generates a clock signal which is a square wave TTL signal having a frequency of twice of the output signal. The next stage, of which logic diagram is presented in Fig. 3, generates two signals for driving the MOSFETs. The rising edge of the clock signal will trigger simultaneously the flip-flop and the monostable. The outputs of the flip-flop will be complementary to each other and the monostable will generate negative-going pulses at its output. The frequency of these signals is half of that of the clock signal. They are the input signals for the two AND gates driving the MOSFETs.

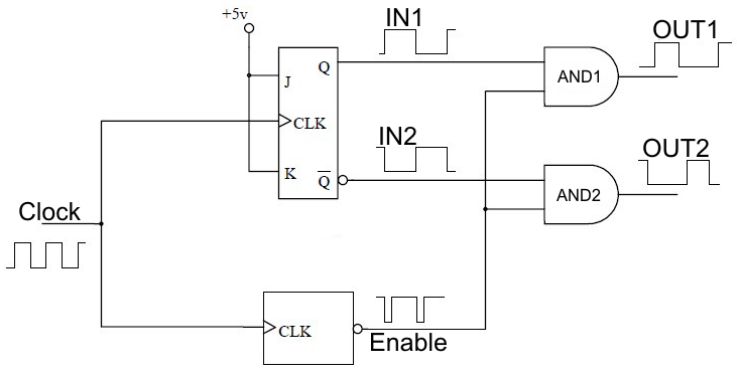

Fig. 3 – Logic diagram of driving signal generator.

Fig. 4 depicts the input/output waveforms of AND gates. As it can be seen, in each period, a time interval equal to twice of the low-state time of the monostable output, neither of the two AND gates has its output in high-state. This time is called “dead-time”. So, by adjusting the high state time of the monostable output, the length of the dead-time and implicitly of the high state of each AND gate output can be controlled. The two driving signals are then fed to the optocoupler stage which separates the high voltage stage from the low voltage driving circuits. The output signals of the optocoupler command the two gate power MOSFET drivers (TC427CPA) having a source and sink capability of 3 A. The gate drivers are mounted closed to each MOSFET in order to obtain a minimum leakage inductance of the circuit.

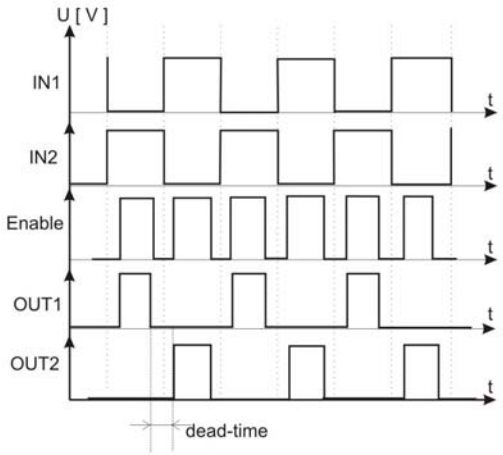

Fig. 4 – Driving signal generator waveforms.

The half-bridge power stage of the inverter was designed to generate the maximum RF power at the running frequency. Because the running frequency is up-limited by the MOSFET capacitances, the transistors must have the gate-source capacitance and the reverse transfer capacitance as low as possible. For minimum dissipation power, the internal distributed gate resistance should be minimal. Another important specification of the MOSFET working as a switch is the capacity to withstand large voltage slew rates when it is turned off. For our application the IRFP450 MOSFET, operating with dc supply voltages in the range of 50-150 V and average currents lower than 1 A, was found to be the most appropriate.

In order to obtain reliable operation of the series resonant inverter and to have clean sinusoidal waveforms, some construction precautions must be considered: (a) the inductance of the gate charging and discharging loop through the gate driver must be of a minimum value by using auxiliary low impedance capacitors placed

near the driver circuits; (b) the stray capacitance added to the midpoint due to the physical construction of the inverter should be kept as low as possible; and (c) the power MOSFETs must be provided with adequate means of thermal dissipation.

2.2. LOAD OF THE INVERTER CIRCUIT

The high-frequency power is fed from the inverter's mid-point through a ferrite core transformer and the Tesla coil to the plasma chamber where it is absorbed by the plasma itself (Fig. 2). The ferrite core transformer magnifies the output voltage of the inverter by a factor of 10. This high voltage is needed to "pump" the base of the Tesla coil in order to generate the high voltage ($\approx 10^1$ kV_{pk}) output RF signal, necessary to generate the atmospheric pressure plasma. The ferrite core transformer's number of primary turns N_p, is derived from the fundamental Faraday law [5]:

$$V_p = kN_p \left(BA_c\right) f \cdot 10^{-8} \tag{1}$$

where: V_p is the primary voltage, k is a shape factor ($k = 4$ for rectangular wave), B is the flux density in gauss, A_c is the cross-sectional area of the core, f is the frequency in Hz and N_p is the number of primary turns.

The secondary voltage V_s is determined by the number of second-winding turns (N_s):

$$V_s = V_p \left(\frac{N_s}{N_p}\right) \tag{2}$$

The Tesla coil was designed as described in [1], so that resonant frequency of the circuit containing the Tesla coil and the plasma chamber to be of 1.71 MHz. This frequency was determined with the help of a circuit formed by a signal generator and an oscilloscope connected through a 1 kΩ resistor (Fig. 5).

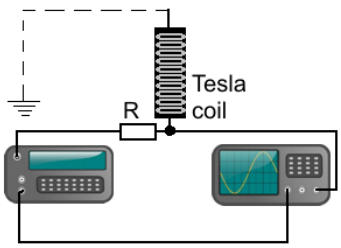

Fig. 5 – The test circuit for determining the Tesla coil's self resonant frequency.

Varying the frequency of the signal generator and watching the waveform on the oscilloscope, we find the resonant frequency when the amplitude of the signal

shows a sudden drop. For the correct operation, the frequency of the inverter must be tuned to be equal with the frequency determined with this method.

2.3. FAULT PROTECTION CIRCUIT

The fault-protection circuit (Fig. 6) has the task to block the drive signals in case the output voltage at the mid-point and/or the load current through the half-bridge exceeds the pre-set values. The signal for the over voltage protection is measured on the resistor R_2, and the over-current signal is determined by the voltage drop on R_s (see Fig. 2). The logic circuit of the fault protection module is built around two high speed comparators LT1016. The protection circuit blocks the drive signals of both high and low sides of the inverter in case any of the voltage or current signals become higher than the reference voltages of the comparators.

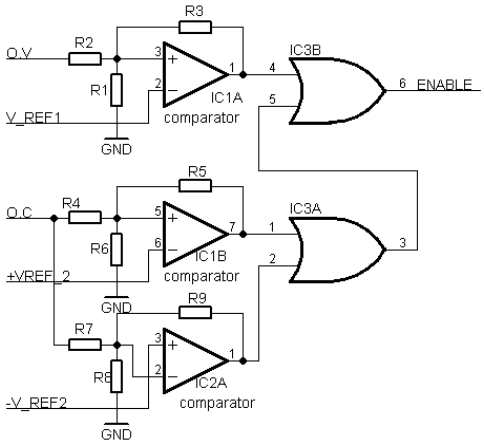

Fig. 6 – Fault-protection circuit logic diagram.

2.4. PLASMA CHAMBER

The plasma reactor chamber (Fig. 7) has a parallelepipedic form with a volume of 160 cm^3. It contains two disk shaped metallic electrodes (24.5 mm diameter) covered with PTFE (1.5 mm thickness) as dielectric. The high of the discharge space can be varied in the range of 0.5-2 cm. One of the electrodes is connected to the Tesla coil output and the other is connected to the inverter's ground. The chamber is closed, having an access nozzle for the plasma gas on one side and two exit holes (3 mm diameter) on the opposite side. The plasma gas (helium with flow-rates lower than 5 l/min) flows perpendicular to the electric field through the discharge space. Small quantities of ambient air can penetrate in the plasma chamber through the two exit holes by back diffusion.

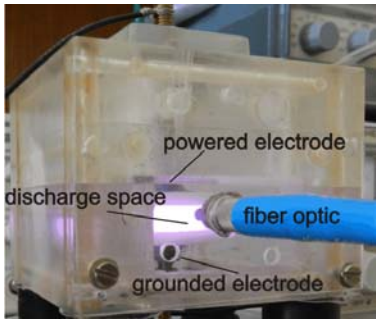

Fig. 7 – Plasma chamber.

3. PLASMA CHARACTERISTICS AND TREATMENT TESTS

A time averaged visual appearance of the discharge is shown in Fig. 8. For fixed values of dc supply voltages ($U_{\pm} = \pm 86$ V , Fig. 2) the discharge is initiated at a helium flow-rate of 0.15 l/min when the light emission from the plasma is visually observed. Initially the plasma has a thin column aspect and covers only small areas of the PTFE dielectrics (filamentary developing stage). The plasma column is surrounded by a region of reduced brightness. With the increase of the gas flow-rate to 1 l/min, both the power absorbed by the discharge and its emission intensity increase, and the plasma column spreads on the dielectrics taking a cylindrical shape with almost the same transversal area as the electrodes (homogeneous stage). The discharge has a white-purplish glow color and appears as a uniform and homogeneous throughout the volume.

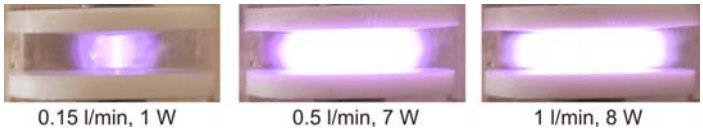

Fig. 8 – Plasma appearance and plasma power as function of helium flow-rate.

A further increase up to 2.8 l/min in the helium flow-rate determines an increasing in the plasma power and its emission. For helium flow-rates higher than 3 l/min the plasma power slightly decreases, probably because of the higher transit velocity of the plasma gas through the inter-electrode space.

The gas kinetic temperature of DBD working in the homogeneous stage (8 W power and 1 l/min helium flow-rate) was of 513 K. It was measured with a K-type thermocouple connected to a multimeter. To avoid the hot junction of the thermocouple to become an extra-electrode of the discharge, it was covered with a cap of Pyrex-glass. Knowing that at atmospheric pressure the rotational temperature of the molecules could be a good approximation of the gas kinetic

temperature, the measured temperature was compared with the rotational temperature of the nitrogen ionic molecule. It was estimated to be of 490 K. It is very close to the temperature measured with the thermocouple.

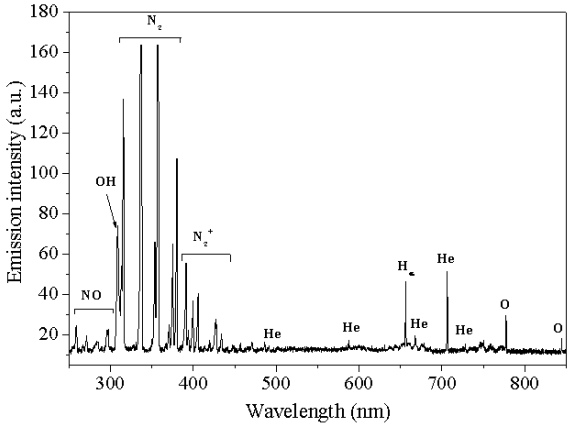

Fig. 9 – Emission spectrum of DBD. Plasma power – 8 W; He flow-rate – 0.5 l/min.

A typical emission spectrum of the helium plasma in the range of 200-900 nm is shown in Fig. 9. Beside the helium emission lines (501.56, 587.56, 667.81, 706.51 and 728.23 nm) as main working gas, atomic emission lines of oxygen (777.41 and 844.67 nm) and hydrogen (656.27 nm) and molecular bands of NO, OH, N_2 and N_2^+ are presented in the radiation spectrum. The presence in the plasma of the other atomic and molecular species than helium is inevitable because of the back diffusion of the ambient air.

The wavelength range of 200-300 nm is dominated by the NO molecular γ-bands (226.28, 236.33, 247.11, 258.75 and 271.32 nm). The presence of NO is due to the chemical conversion of N_2 and O_2. It follows the emission band of OH radical at 308.9 nm. The OH radicals represent the result of the dissociation of H_2O molecules from the humid back diffused air caused by the collisions with the energetic electrons or with long life species presented in the plasma, especially with helium metastables, He_m^*. Beginning with the wavelength of 315 nm the UV spectrum is dominated by the emission of nitrogen molecules, the most representative being: the emissions of 2nd positive system of N_2 (315.93, 337.13, 357.69 and 380.49 nm) and of 1st negative system of N_2^+ (391.44 nm). It must be mentioned here that the N_2^+ emission is attributed to Penning ionization of N_2 with helium metastables. Otherwise it is well known that nitrogen molecules are very effective at quenching the helium metastables. The presence of the basic atomic line of hydrogen, H_α, is due to the excitation of hydrogen atoms generated by dissociation of H_2O molecules.

The presence of the electrons and of the atomic, ionic and molecular active species in the helium DBD is important from the point of view of possible applications of this kind of plasma, especially in the surfaces treatment and bacterial inactivation. By observing the effect of the plasma on the tracing paper, PET and glass wettability, the possibility of using the generated DBD in the surface treatment was tested. 3 μl of bi-distilled water droplets as test liquid were deposited on the surfaces using a pipette. The photos of each droplet deposited on the untreated and treated surfaces respectively, were taken using a digital camera (Fig. 10). As it can be seen, after only one second of exposure time, the effect of the plasma treatment on the wettability (associated with the contact angle) is very visible. The images were processed by *Image J* free software [6] using the contact angle plugin [7].

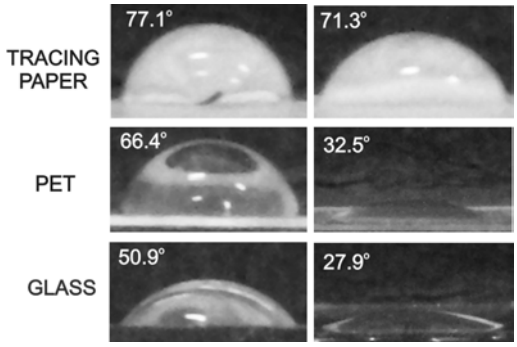

Fig. 10 – Photographs and the corresponding contact angles of water droplets deposited on different untreated and treated surfaces (treatment time – 1 s, plasma power – 8 W, He flow-rate – 0.5 l/min).

4. CONCLUSIONS

A laboratory-made, inverter based cold plasma generator circuit was investigated. It was found that a half-bridge type inverter is the most suitable topology for this kind of application. The main practical problems of implementing a half-bridge inverter were found to be the generation of the control signals, the gate-drive circuits and the physical construction of the inverter output stage. Preliminary studies on the generated plasma have shown that for a fixed value of symmetric dc supply voltages, the characteristics of the generated DBD (plasma volume, absorbed power, gas temperature and plasma emission) are dependent on the He flow-rate. The plasma was successfully used to increase the hydrophilicity of several materials.

Acknowledgements. This study was supported by National University Research Council, Ministry of Education, Research and Innovation, Romania, Grant PN II-PCE 446/2009, code ID_2270.

REFERENCES

1. C.D. Tudoran, *Simplified portable 4 MHz RF plasma demonstration unit*, J Physics: Conference Series **182,** 012034 (2009).
2. S.D. Anghel, *Generation and Electrical Diagnostic of an Atmospheric-Pressure Dielectric Barrier Discharge*, IEEE Trans. Plasma Sci. **39**, 871–876 (2011).
3. S.D. Anghel, *Generation and investigation of a parallel-plate DBD driven at 1.6 MHz with flowing helium*, J. Electrost., **69**, 261–264 (2011).
4. P.J. Baxandall, *Transistor sine-wave LC ocillators*, Proc. IEEE Suppl., **106B**, 748–758 (1959).
5. W. F. Smith, *An overview of Faraday's Law*, Haverford College 6-5-02, can be found at: http://www.haverford.edu/physics/songs/faraday_hi _story.pdf.
6. W. Rasband, *ImageJ*, version 1.42, National Institute of Health, 2009, can be found at: http://rsbweb.nih.gov/ij/index.html
7. M. Brugnara, *Contact Angle plugin* (for *ImageJ* software), 2006, can be found at: http://rsbweb.nih.gov/ij/plugins/ contact-angle.html